A Novel Feedforward Hybrid Active Noise Control System with Narrowband Frequency Adaptive Estimation and Error Separation

*PANG Mingrui, LIU Yifei, LIU Jian**

College of Automation Engineering, Nanjing University of Aeronautics and Astronautics, Nanjing 211106, P. R. China

(Received 25 December 2024; revised 6 June 2025; accepted 10 September 2025)

Abstract: The conventional feedforward hybrid active noise control (FFHANC) system combines the advantages of the feedforward narrowband active noise control (FFNANC) system and the feedforward broadband active noise control (FFBANC) system. To enhance its adaptive adjustment capability under frequency mismatch (FM) conditions, this paper introduces a narrowband frequency adaptive estimation module into the conventional FFHANC system. This module integrates an autoregressive (AR) model and a linear cascaded adaptive notch filter (LCANF), enabling accurate reference signal frequency estimation even under significant FM. Furthermore, in order to improve the coherence between narrowband and broadband components in the system's error signal and its corresponding control filter for the conventional FFHANC system, this paper proposes an algorithm based on autoregressive bandpass filter bank (AR-BPFB) for error separation. Simulation results demonstrate that the proposed FFHANC system maintains robust performance under high FM conditions and effectively suppresses hybrid-band noise. The AR-BPFB algorithm significantly elevates the convergence speed of the FFHANC system.

Key words: active noise control; feedforward hybrid active noise control (FFHANC) system; autoregressive (AR) model; linear cascaded adaptive notch filter (LCANF); bandpass filter bank (BPFB); error separation

CLC number: TN 911.7 **Document code:** A **Article ID:** 1005-1120(2025)05-0638-10

0 Introduction

Since the 1970's, the development of active noise control (ANC) has been attempted in force to reduce the low-frequency noise level(<1 kHz) and extensive system structures, and adaptive algorithms have been developed[1-5]. The adaptive filtering schemes are widely studied and used to generate the anti-noise wave.

Based on the linearity of their input-output mathematical models, ANC systems can be classified as either linear ANC system or nonlinear system. Due to low computational cost, structural simplicity, and strong stability, most existing ANC systems are mainly linear ANC systems composed of finite impulse response (FIR) filters[1-3] and adjusted by the filtered-x least mean square (FxLMS) algorithm and its variants. In contrast, nonlinear ANC systems are only considered for complex nonlinear noise characterized by short duration, high amplitude, or irregular frequency variations, such as impulse noise or nonlinear distortion etc[6-9].

Based on noise control strategies, linear ANC systems are primarily classified into three categories, feedforward ANC (FFANC)[10-12], feedback ANC (FBANC)[13-14], and hybrid ANC (HANC)[15-16] that combines FFANC and FBANC. FFANC[1] systems can be divided into feedforward broadband ANC (FFBANC) system and feedforward narrowband ANC (FFNANC) system based on the way of obtaining reference signals. The FFBANC sys-

*Corresponding author, E-mail address: jliu@nuaa.edu.cn.

How to cite this article: PANG Mingrui, LIU Yifei, LIU Jian. A novel feedforward hybrid active noise control system with narrowband frequency adaptive estimation and error separation[J]. Transactions of Nanjing University of Aeronautics and Astronautics, 2025, 42(5): 638-647.

http://dx.doi.org/10.16356/j.1005-1120.2025.05.007

tem is widely used thanks to its robust performance and simple architecture. However, its effectiveness diminishes in scenarios requiring fast convergence, particularly when handling mixed broadband-narrowband noise components, which has led to the proposal of feedforward hybrid active noise control (FFHANC) system[17].

Since the proposal of the FFHANC system, efforts have been made to improve its performance[18-23]. A key focus is to address the frequency mismatch (FM) issue between the measured and actual reference signal frequencies. In FFNANC systems, the reference signal generator typically uses two types of reference signals[1], pulse sequences and sine waves. The first technique is called waveform synthesis, triggered by synchronous pulses from non-acoustic sensors. The second technique typically uses adaptive notch filter (ANF) to suppress or extract harmonic signals of specific frequencies[1]. Xiao et al.[18] proposed a second-order autoregressive (AR) recursive algorithm for frequency tracking of sine reference signals and verified its effectiveness under low FM conditions (2%). Based on the above research, a linear cascaded adaptive notch filter-AR (LCANF-AR) combination method was developed in Ref.[24], which performed well in high FM (25%) scenarios without the need for initial frequency information. It is worth noting that the ANF strategy[23] is rarely applied to FFHANC systems. Therefore, in this study, we applied the LCANF-AR algorithm from Ref.[24] within the conventional FFHANC framework established in Ref.[17], and evaluated its ability to improve the noise reduction performance of FFHANC systems under high FM conditions.

Furthermore, theoretical analysis indicates that in FFNANC systems, the residual error components from other channels can reduce the convergence speed of each adaptive filter[25]. Therefore, when studying FFHANC systems, attention must also be paid to the coupling of error signals between subsystems. Refs.[26—29] have investigated and applied various error separation structures and algorithms for FFHANC or HANC systems. The mainstream approach involves extracting narrowband error components from the total error signal with broadband components left. Chang et al.[25] proposed a complete parallel error separation algorithm based on a set of second-order infinite impulse response (IIR) zero-delay bandpass filter bank (BPFB) structure from Ref.[30]. Although this algorithm has been verified to improve the convergence speed of FFNANC systems, it requires the introduction of additional adaptive recursive processes. Xiao[31] introduced another type of BPFB with constrained zeros and poles (CZP-BPFB[32]) to obtain more accurate filtered-x signals for FFNANC systems. Subsequently, an AR model was incorporated into the system, and the transfer function of the BPFB was updated by replicating its frequency correlation coefficient. Similarly, Wang et al.[27] used the BPFB structure from Ref.[32] for error separation in their study of HANC systems, further enhancing the performance and robustness of the HANC system. But the computational load of the proposed system still needs to be reduced. Inspired by the above studies, this paper proposes an autoregressive bandpass filter bank algorithm (AR-BPFB) for error separation, which incorporates an AR-model-parameter-based update mechanism for its time-varying transfer function[30], along with its derived computational procedure. This approach significantly reduces computational complexity while achieving faster convergence speeds.

In light of the improvements aforementioned, this paper proposes a novel FFHANC system with narrowband frequency adaptive estimation and error separation. The remainder of the paper is organized as follows: Section 1 provides a comprehensive overview of the conventional FFHANC system. Sections 2 presents the proposed FFHANC system. Complexity analysis is given in Section 3. Section 4 presents the results of a simulation that assesses the comprehensive performance of the proposed FFHANC system. Section 5 provides a summary of the paper.

1 Conventional FFHANC System

The conventional FFHANC system[17] includes following components. It contains the sinusoidal noise canceller (SNC) subsystem, the FFBANC and FFNANC subsystem. The former adopts the least mean square (LMS) algorithm for its adaptive filter, and the latter two adopt the FxLMS algorithm. The overall configuration is shown in Fig.1.

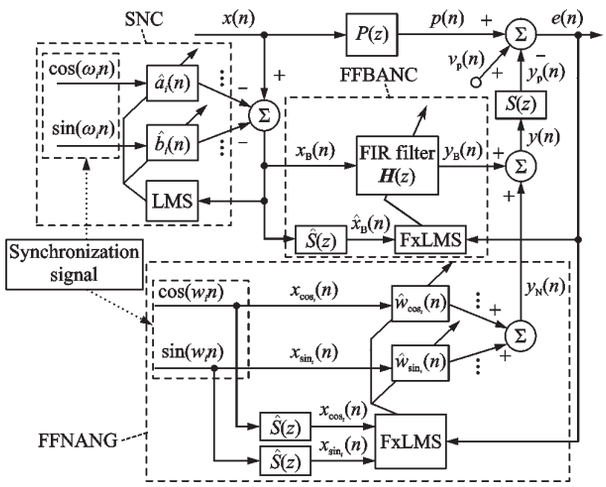

Fig.1 Conventional FFHANC system

The primary path, secondary path and estimate models of secondary path are expressed as

$$\begin{cases} P(z)=\sum_{j=1}^{M_P} p_j z^{-j} \\ S(z)=\sum_{j=1}^{M} s_j z^{-j} \\ \hat{S}(z)=\sum_{j=1}^{\hat{M}} \hat{s}_j z^{-j} \end{cases} \tag{1}$$

where $M_P, M, \hat{M}$ are the FIR model orders and $p_j, s_j, \hat{s}_j$ the impulse responses of $P(z), S(z)$ and $\hat{S}(z)$, respectively; $P(z)$ indicates the primary-path transfer function from the reference sensor to the error sensor, $S(z)$ the secondary-path transfer function from the cancelling speaker to the error sensors; and $\hat{S}(z)$ the estimate of $S(z)$ which can be obtained by offline or online secondary-path modeling. The total reference signal is given as

$$\begin{cases} x(n)=x_{\mathrm{N}}(n)+x_{\mathrm{B}}(n)= \\ \qquad \sum_{i=1}^{q}[A_i x_{\cos_i}(n)+B_i x_{\sin_i}(n)]+x_{\mathrm{B}}(n) \\ x_{\cos_i}(n)=\cos(w_i n), x_{\sin_i}(n)=\sin(w_i n) \end{cases} \tag{2}$$

where n denotes the discrete time index; and $x_{\mathrm{N}}(n)$ and $x_{\mathrm{B}}(n)$ represent the narrowband and the broadband components, respectively. $x_{\mathrm{N}}(n)$ comprises a set of cosine signals $\{x_{\cos_1}(n), x_{\cos_2}(n), \cdots, x_{\cos_i}(n)\}$ $(i=q)$ and sinusoidal signals $\{x_{\sin_1}(n), x_{\sin_2}(n), \cdots, x_{\sin_i}(n)\}(i=q)$ that are commonly derived from synchronization signals. $\{A_1, A_2, \cdots, A_i\}(i=q)$ and $\{B_1, B_2, \cdots, B_i\}$ $(i=q)$ represent the amplitudes of the cosine signals and the sinusoidal signals, respectively. i represents the ith frequency while q the total number of frequencies; $\{w_1, w_2, \cdots, w_i\}(i=q)$ the angular frequency corresponding to the ith frequency. Here, angular frequency $w_i=2\pi f_i/f_{\mathrm{s}}$, where f_i is the frequency of the ith component of $x_{\mathrm{N}}(n)$ and f_{s} the sampling rate; and $x_{\mathrm{B}}(n)$ a zero-mean white or colored noise with variance σ_w^2. The primary noise is expressed as

$$p(n)=v_{\mathrm{p}}(n)+\sum_{j=0}^{M_P-1} p_j(j+1)x(n-j) \tag{3}$$

where $v_{\mathrm{p}}(n)$ is the additive Gaussian white noise whose statistical characteristics are completely independent of the reference signal $x(n)$.

The secondary noise signal $y_{\mathrm{p}}(n)$ used to cancel the primary noise is generated by filtering the output $y(n)$ through the secondary channel $S(z)$

$$\begin{cases} y(n)=y_{\mathrm{B}}(n)+y_{\mathrm{N}}(n) \\ y_{\mathrm{p}}(n)=\sum_{j=0}^{M-1} s_j y(n-j) \end{cases} \tag{4}$$

where $y_{\mathrm{B}}(n)/y_{\mathrm{N}}(n)$ is the output signal (i.e. secondary source signal) of the FFNANC/FFBANC subsystem, which will be given later. Thus, the total error signal can be represented as

$$e(n)=p(n)-y_{\mathrm{p}}(n) \tag{5}$$

1.1 FFNANC subsystem

The narrowband components in the primary noise $x(n)$ are compensated by a typical FFNANC subsystem[1] which is a linear combiner with two

control filter weights for each targeted frequency. Its output signal is given as

$$\begin{cases} y_{\mathrm{N}_i}(n)=w_{\cos_i}(n)x_{\cos_i}(n)+w_{\sin_i}(n)x_{\sin_i}(n) \\ y_{\mathrm{N}}(n)=\sum_{i=1}^{q}y_{\mathrm{N}_i}(n) \end{cases} \tag{6}$$

The FxLMS algorithm is used to update the control filter weights.

$$\begin{cases} w_{\cos_i}(n+1)=w_{\cos_i}(n)+\mu_{\mathrm{N}}e(n)\hat{x}_{\cos_i}(n) \\ w_{\sin_i}(n+1)=w_{\sin_i}(n)+\mu_{\mathrm{N}}e(n)\hat{x}_{\sin_i}(n) \end{cases} \tag{7}$$

where μ_{N} is the step size of the adaptive filter of FFNANC subsystem; and $\hat{x}_{\cos_i}(n)$, $\hat{x}_{\sin_i}(n)$ are the filtered-x reference signals filtered by $\hat{S}(z)$

$$\begin{cases} \hat{x}_{\cos_i}(n)=\sum_{j=0}^{\hat{M}-1}\hat{s}_j x_{\cos_i}(n-j) \\ \hat{x}_{\sin_i}(n)=\sum_{j=0}^{\hat{M}-1}\hat{s}_j x_{\sin_i}(n-j) \end{cases} \tag{8}$$

1.2 FFBANC subsystem

The FFBANC system adopts the standard FxLMS algorithm for filtering. However, the number of controller coefficients becomes very large and depends on various parameters such as the frequency bandwidth of the disturbance signal[33].

Its output signal $y_{\mathrm{B}}(n)$ and update function of control filter weights $\boldsymbol{H}(n)$ are respectively given by

$$\begin{cases} y_{\mathrm{B}}(n)=\boldsymbol{H}^{\mathrm{T}}(n)\hat{\boldsymbol{x}}_{\mathrm{B}}(n)=\sum_{j=0}^{L_{\mathrm{B}}-1}H_j(n)\hat{x}_{\mathrm{B}}(n-j) \\ \boldsymbol{H}(n+1)=\boldsymbol{H}(n)+\mu_{\mathrm{B}}\hat{\boldsymbol{x}}_{\mathrm{B}}(n)e(n) \end{cases} \tag{9}$$

where L_{B} is the length of the broadband adaptive filter coefficients vector $\boldsymbol{H}(n)$; $H_j(n)$ the jth coefficient of $\boldsymbol{H}(n)$; $\hat{x}_{\mathrm{B}}(n)$ the broadband component in $x(n)$ filtered by $\hat{S}(z)$; and $\hat{\boldsymbol{x}}_{\mathrm{B}}(n)$ the vector comprised by $\hat{x}_{\mathrm{B}}(n)$ from the present and past $L_{\mathrm{B}}-1$ time points.

1.3 SNC subsystem

As is illustrated in Fig.1, the SNC includes a discrete Fourier analyzer which can effectively separate narrowband signals out. Therefore, the reference signal of the FFBANC subsystem $x_{\mathrm{B}}(n)$ can be obtained by subtracting the sum of estimated reference signal of the FFNANC system $\hat{x}_{\mathrm{N}_i}(n)$ from $x(n)$

$$\begin{cases} x_{\mathrm{B}}(n)=x(n)-\hat{x}_{\mathrm{N}}(n) \\ \hat{x}_{\mathrm{N}}(n)=\sum_{i=1}^{q}[\hat{a}_i(n)x_{\cos_i}+\hat{b}_i(n)x_{\sin_i}] \end{cases} \tag{10}$$

Similarly, the FxLMS algorithm is used to update the SNC controller weight coefficients $\hat{a}(n)$ and $\hat{b}(n)$.

$$\begin{cases} \hat{a}_i(n+1)=\hat{a}_i(n)+\mu_c e_i(n)x_{\cos_i}(n) \\ \hat{b}_i(n+1)=\hat{b}_i(n)+\mu_c e_i(n)x_{\sin_i}(n) \end{cases} \tag{11}$$

The variable step size parameter $\mu_c(n)$ is calculated as

$$\begin{cases} \mu_c(n)=\alpha\mu_c(n-1)+(1-\alpha)\mu_{c,\min} \\ \mu_c(0)=\mu_{c,\max} \end{cases} \tag{12}$$

where α is a constant defined within $(0,1]$; $\mu_{c,\max}$ the maximum or initial value of the step size which is set to a large value such that the SNC converges fast enough in the early stage of adaptation; $\mu_{c,\min}$ the minimum or steady-state value which is set small to guarantee the steady-state performance of the SNC.

2 The Proposed FFHANC System

The structure of the proposed FFHANC system is shown in Fig.2. The system incorporates two key improvements on the basis of the conventional FFHANC framework.

(1) Adopt the frequency adaptive estimation module proposed in Ref.[24] which integrates AR model and LCANF.

(2) Adopt the narrowband error signal separation module based on the BPFB structure proposed in Ref.[25], and propose the AR-BPFB algorithm to adaptively update passband center frequencies of BPFB. Derive the calculation process.

Similarly, by subtracting the separated multichannel narrowband error signals from the total error signal, the broadband error signal is obtained, thereby achieving effective error signal decoupling.

In addition, the second-order AR model can generate synchronous reference signals for SNC subsystem, thereby improving the accuracy and stability of reference signal separation.

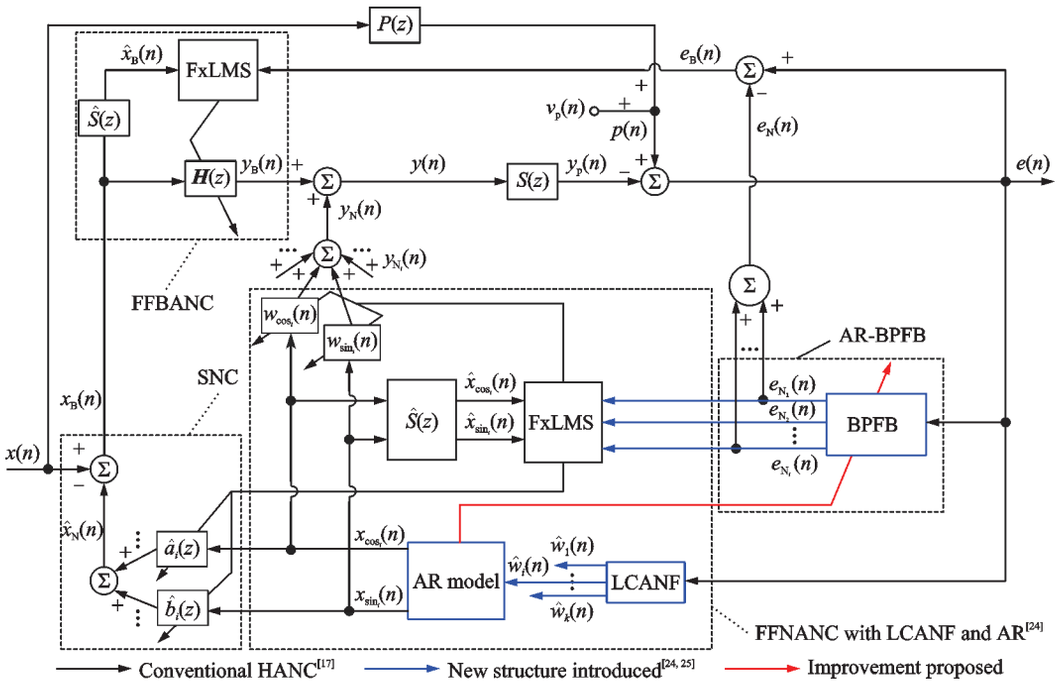

Fig.2 Proposed FFHANC system

The BPFB structure is constructed by a set of second-order IIR-type bandpass filters (BPFs) to extract the narrowband errors $\{e_{N_i}(n)\}_{i=1}^{k}$ corresponding to the respective narrowband frequency channels from the total error signal $e(n)$.

A classical second-order IIR-type BPF time invariant transfer function[30] is given by

$$h_i(z)=\frac{(1-p_i^2)\left(\frac{q_i z}{1+p_i^2}-1\right)}{z^2-q_i z+p_i^2} \tag{13}$$

where the value of $p_i(0\leqslant p_i<1)$ is related to the bandwidth of the filter. Parameter $q_i(|q_i|\leqslant 2p_i)$ affects the value of passband center frequency f_i

$$f_i=\frac{f_s}{2\pi}w_i=\frac{f_s}{2\pi}\arccos\left(\frac{q_i}{1+p_i^2}\right) \tag{14}$$

In practical applications, f_i is usually time-varying so the fixed parameter q_i turns into a time-varying parameter $q_i(n)$. Therefore, Eqs.(13, 14) can be updated as dynamic transfer function

$$f_i(n)=\frac{f_s}{2\pi}\omega_i(n)=\frac{f_s}{2\pi}\arccos\left(\frac{q_i(n)}{1+p_i^2}\right) \tag{15}$$

$$h_i(z,n)=\frac{(1-p_i^2)\left(\frac{q_i(n)z}{1+p_i^2}-1\right)}{z^2-q_i(n)z+p_i^2} \tag{16}$$

Then, the relationship between $e(n)$ and $\{e_{N_i}(n)\}_{i=1}^{k}$ can be expressed as

$$\begin{cases} e_{N_i}(n)=e'(n)-e'_{N_i}(n) \\ e'(n)=\dfrac{1-p_i^2}{1+p_i^2}q_i(n)e(n-1)-(1-p_i^2)e(n-2) \\ e'_{N_i}=-q_i(n)e_{N_i}(n-1)-p_i^2e_{N_i}(n-2) \end{cases} \tag{17}$$

Then, the relationship between two subsystem error signals $e_N(n)$, $e_B(n)$ and the total system error signal $e(n)$ are expressed as

$$\begin{cases} e_N(n)=\sum_{i=0}^{k}e_{N_i}(n) \\ e_B(n)=e(n)-e_N(n) \end{cases} \tag{18}$$

In Ref.[24], the conversion formula between AR model parameters and target tracking frequency is given by

$$w_i(n)=\arccos\left(\frac{c_i(n)}{-2}\right) \tag{19}$$

Eq.(15) and Eq.(19) have the same format, so the BPF parameter $q_i(n)$ can be transferred by the AR model parameter $c_i(n)$. The relationship between the two parameters is as

$$q_i(n)=\frac{1+p_i^2}{-2}c_i(n) \tag{20}$$

The principle of proposed method is shown in Fig.3.

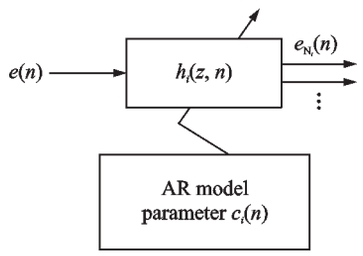

Fig.3 BPFB parameter adjustment principle

After the adjustment, the BPFB structure can adaptively track the dominant noise frequency using the AR model without introducing additional adaptive recursive algorithms, significantly reducing computational complexity.

3 Complexity Analysis

Computational complexity is essential to assess a newly proposed system. The complexity analysis in one iteration of the conventional FFHANC system, the proposed FFHANC system, and the modules for frequency adaptively estimation and error separation are listed in Table 1. Here, for the convenience of comparison, we assume that lengths of primary path, secondary path and estimated secondary path are all M. N_{anf} is the estimated sample size used to control the participation of the LCANF and AR model[24].

Table 1 Computational complexity per-iteration of FFHANC systems and modules

System	Multiplications	Additions
AR ($N>N_{\text{anf}}$)	$2q$	$2q$
LCANF ($N\leqslant N_{\text{anf}}$)	$8q$	$6q$
BPFB[25] ($N>N_{\text{anf}}$)	$11q$	$7q$
BPFB[32] ($N>N_{\text{anf}}$)	$7q+2$	$6q+2$
Proposed AR-BPFB ($N>N_{\text{anf}}$)	$6q$	$3q$
Conventional FFHANC[17]	$3L_{\text{B}}+(2q+3)M+8q+6$	$2L_{\text{B}}+(2q+3)M+8q+2$
Proposed FFHANC ($N\leqslant N_{\text{anf}}$)	$L_{\text{B}}+(2q+3)M+12q$	$L_{\text{B}}+(2q+3)M+10q+1$
Proposed FFHANC ($N>N_{\text{anf}}$)	$3L_{\text{B}}+(2q+3)M+16q+6$	$2L_{\text{B}}+(2q+3)M+13q+2$

The proposed AR-BPFB algorithm significantly reduces the computational cost of error separation by eliminating $5q/(q+2)$ multiplications and $4q/(3q+2)$ additions, compared to the conventional method in Refs.[25, 27]. Furthermore, the proposed FFHANC system demonstrates approximately $2L_{\text{B}}$ lower computational costs in the frequency estimation stage ($N\leqslant N_{\text{anf}}$) than those in the denoising stage ($N>N_{\text{anf}}$), while maintaining a relatively low overall computational burden. After completing the frequency estimation, the proposed system consumes only $8q$ more multiplications and $5q$ more additions (from introduced AR&AR-BPFB) in total than those of the conventional FFHANC system. These additional computational loads are tolerable and can be offset by the improved stability and noise reduction performance.

4 Computer Simulation

In this section, we conduct extensive MATLAB simulations to validate the superior noise suppression performance of the proposed FFHANC system under high FM conditions, as well as that of the AR-BPFB algorithm for error signal separation. Simulation conditions are as follows. Sampling points N: 8 000. Sampling frequency f_{s}: 4 kHz. Primary path $P(z)$: Generated by function fir1 (M_P=61, cutoff frequency w_{cf}=0.6π). Secondary path $S(z)$: Generated by function fir1 (M=31, cutoff frequency w_{cf}=0.6π). $\hat{S}(z)$: The estimate of $S(z)$ that is modeled through offline identification in advance by LMS algorithm ($\hat{M}$=41). Narrowband noise component: Sinusoids (q=3, $\{A_1, A_2, A_3\}=\{1, 1, 1\}$, $\{w_1, w_2, w_3\}=\{0.05\pi, 0.10\pi, 0.15\pi\}$. Broadband noise component: Band-limited Gaussian white noise in $x(n)$ with variance $\sigma_{\text{B}}^2=1$. Band-

width ranges from 500 Hz to 1 000 Hz. AR model step size: $\{\mu_{\text{anf}_1}, \mu_{\text{anf}_2}, \mu_{\text{anf}_3}\} = \{0.000\,2, 0.000\,1, 0.000\,1\}$. LCANF step size: $\{\mu_{\text{anf}_1}, \mu_{\text{anf}_2}, \mu_{\text{anf}_3}\} = \{0.000\,2, 0.002\,5, 0.003\}$. ANF polar radius parameter: $r_i = 0.98$. FFANAC parameters: $\mu_{\text{N}} = 0.02$. SNC parameters: $\mu_{\text{snc}} = 0.05$, $\alpha = 0.975$, $\mu_{c,\min} = 0.05$, $\mu_{c,\max} = 1 - \mu_{c,\min}$. FFBANC parameters: $L_{\text{B}} = 32$, $\mu_{\text{B}} = 0.01$. BPFB constant: $p_i = 0.97$.

In simulation experiments, it is necessary to quantitatively evaluate the performance of adaptive algorithms. This study adopts the mean squared error (MSE) of the system at time n as the measurement standard, which is defined as

$$\text{MSE}(n) = E(e^2(n)) \tag{21}$$

To ensure statistical reliability, according to MonteCarlo method, the simulation results are averaged over T independent computer simulation runs (taken as 1 500)

$$\text{MSE}(T,n) = 10\lg\left(\frac{1}{T}\sum_{t=0}^{T} e_t^2(n)\right) \tag{22}$$

where $e_t(n)$ is the error siganl at iteration n for the tth simulation run.

To begin with, Figs.4—5 present the MSE curves of the conventional FFHANC and the proposed FFHANC system under varying FM conditions (2%, 10%, 25%).

The experimental results demonstrate that the conventional FFHANC system achieves satisfactory noise cancellation performance under 2% FM conditions, primarily due to the frequency tracking

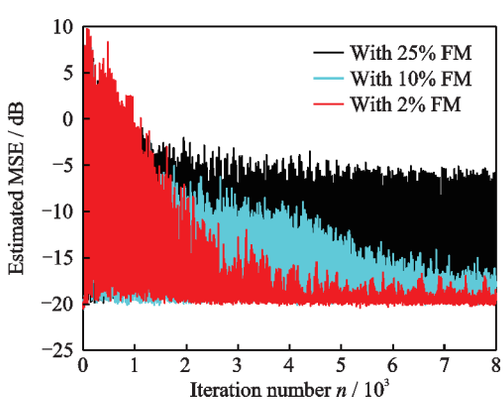

Fig.4 MSE curves obtained by FFHANC system with only AR[18] under different FM conditions

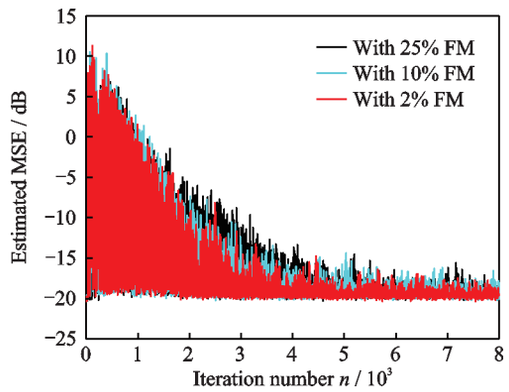

Fig.5 MSE curves obtained by proposed FFHANC system with LCANF and AR in Ref.[24] under different FM conditions

capability of the AR model. However, as the FM level increases to 10% and 25%, both the noise reduction effect and convergence speed of the conventional FFHANC system degrade significantly. Nevertheless, since the FFBANC subsystem possesses the ability to suppress narrowband components to some extent, the system does not diverge.

In contrast, the proposed FFHANC system incorporating the LCANF maintains robust noise cancellation performance and fast convergence across all tested FM conditions. These experimental findings confirm that the integration of LCANF with conventional FFHANC architecture effectively strengthens system robustness against frequency mismatch variations.

Next, Fig.6 presents a comparative analysis of error separation methods for enhancing the convergence speed of FFHANC systems. Specifically, we compare the conventional BPFB method[25, 27] with the proposed AR-BPFB algorithm. Parameter settings have been provided at the start of this section. Fig.5 shows that FM only impacts the system's convergence speed, not its trend. Hence, FM is set to 0% here to eliminate interference.

The results demonstrate that the conventional BPFB method provides a moderate improvement in convergence speed, with the approach in Ref.[27] outperforming that in Ref.[25]. The proposed method delivers a significantly greater enhancement for FFHANC system, which is more important.

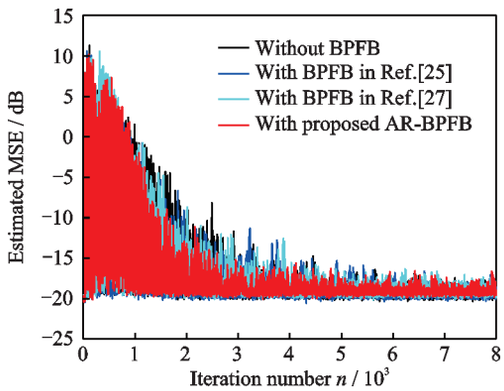

Fig.6 Residual error powers obtained by proposed FFHANC system with different BPFB methods

5 Conclusions

To further enhance the noise reduction performance and robustness of conventional FFHANC system, this study introduces two key improvements: The narrowband frequency adaptive estimation module from Ref.[24], and the narrowband error signal separation module based on the BPFB structure proposed in Ref.[25]. Then this study proposes the AR-BPFB algorithm to adaptively update passband center frequencies of BPFB. These enhancements are systematically incorporated into the conventional FFHANC framework and proposes a novel FFHANC system with narrowband frequency adaptive estimation and error separation. Simulation results demonstrate that the proposed FFHANC system exhibits faster convergence speed and stronger resistance to FM compared to conventional FFHANC systems.

References

[1] KUO S M, MORGAN D R. Active noise control: A tutorial review[J]. Proceedings of the IEEE, 1999, 87(6): 943-973.

[2] KUO S M, MORGAN D R. Active noise control systems, algorithms and DSP implementations[M]. New York, USA: Wiley, 1996.

[3] LU L, YIN K L, DE LAMARE R C, et al. A survey on active noise control in the past decade—Part Ⅰ: Linear systems[J]. Signal Processing, 2021, 183: 108039.

[4] ELLIOTT S. Signal processing for active control[M]. San Diego, USA: Elsevier Science & Technology, 2001.

[5] PANG Y H, OU S F, CAI Z R, et al. Posterior error energy minimization based combined FxNLMS and FxLMS algorithm for active noise control[J]. IEEE Access, 2024, 12: 30754-30764.

[6] GEORGE N V, PANDA G. Advances in active noise control: A survey, with emphasis on recent nonlinear techniques[J]. Signal Processing, 2013, 93(2): 363-377.

[7] LU L, YIN K L, DE LAMARE R C, et al. A survey on active noise control in the past decade—Part Ⅱ: Nonlinear systems[J]. Signal Processing, 2021, 181: 107929.

[8] LI Y D, HE H M, LIU Y, et al. Robust PBFD nonlinear filtering scheme for active noise cancellation with remote acoustic sensing[J]. IEEE Access, 2024, 12: 123476-123488.

[9] CHIEN Y R, YU C H, TSAO H W. Affine-projection-like maximum correntropy criteria algorithm for robust active noise control[J]. IEEE/ACM Transactions on Audio, Speech and Language Processing, 2022, 30: 2255-2266.

[10] SHI D Y, GAN W S, LAM B, et al. Feedforward selective fixed-filter active noise control: Algorithm and implementation[J]. IEEE/ACM Transactions on Audio, Speech and Language Processing, 2020, 28: 1479-1492.

[11] LANDAU I D, MELENDEZ R, AIRIMITOAIE T B, et al. Beyond the delay barrier in adaptive feedforward active noise control using Youla-Kučera parametrization[J]. Journal of Sound and Vibration, 2019, 455: 339-358.

[12] MENG H, CHEN S M. A modified adaptive weight-constrained FxLMS algorithm for feedforward active noise control systems[J]. Applied Acoustics, 2020, 164: 107227.

[13] MA Y P, XIAO Y G, HUANG B Y, et al. A robust feedback active noise control system with online secondary-path modeling[J]. IEEE Signal Processing Letters, 2022, 29: 1042-1046.

[14] AKHTAR M T. Narrowband feedback active noise control systems with secondary path modeling using gain-controlled additive random noise[J]. Digital Signal Processing, 2021, 111: 102976.

[15] WANG Z J, XIAO Y G, MA Y P, et al. A new hybrid active noise control system with input-power-controlled online secondary-path modeling[J]. IEEE/ACM Transactions on Audio, Speech, and Language

Processing, 2024, 32: 3157-3170.

[16] PADHI T, CHANDRA M, KAR A, et al. A new adaptive control strategy for hybrid narrowband active noise control systems in a multi-noise environment[J]. Applied Acoustics, 2019, 146: 355-367.

[17] XIAO Y, WANG J. A new feedforward hybrid active noise control system[J]. IEEE Signal Processing Letters, 2011, 18(10): 591-594.

[18] XIAO Y, WEI H. A feedforward hybrid active noise control system in the presence of sensor error[C]// Proceedings of the 2012 International Conference on Control, Automation, Robotics and Vision (ICARCV). Guangzhou, China: IEEE, 2012.

[19] XIAO Y, DOI K. A robust hybrid active noise control system using IIR notch filters[J]. International Journal of Advanced Mechatronic Systems, 2013, 5(1): 69.

[20] ZHU W Z, LUO L, CHRISTENSEN M G, et al. A new feedforward hybrid active control system for attenuating multi-frequency noise with bursty interference[J]. Mechanical Systems and Signal Processing, 2020, 144: 106859.

[21] MA Y P, XIAO Y G, MA L Y, et al. A robust feedforward hybrid active noise control system with online secondary-path modelling[J]. IET Signal Processing, 2023, 17(1): e12183.

[22] CHEN W, LU C H, LIU Z E, et al. A novel feedforward hybrid active sound quality control algorithm for both narrowband and broadband sound-profiling[J]. Applied Acoustics, 2021, 180: 108095.

[23] BAI T, KIJIMOTO S, ISHIKAWA S, et al. A new feedforward hybrid active noise control system using an adaptive Notch filter bank and its application to fan noise[J]. Applied Acoustics, 2025, 231: 110492.

[24] LIU J, WANG Z X. A narrowband active noise control system with autoregressive model and linear cascaded adaptive Notch filter[J]. Signal Processing, 2022, 196: 108502.

[25] CHANG C Y, KUO S M. Complete parallel narrowband active noise control systems[J]. IEEE Transactions on Audio, Speech, and Language Processing, 2013, 21(9): 1979-1986.

[26] WEN L, HUANG B Y, MA F, et al. A new hybrid active noise control system with residual error separation structure[C]//Proceedings of the Signal and Information Processing Association Annual Summit and Conference (APSIPA), 2014 Asia-Pacific. Siem Reap, Cambodia: IEEE, 2014: 1-4.

[27] WANG Z, XIAO Y, MA Y, et al. A new robust hybrid active noise control system[C]//Proceedings of the 2023 8th International Conference on Signal and Image Processing (ICSIP). Wuxi, China: IEEE, 2023: 742-747.

[28] JIANG Y, CHEN S M, GU F H, et al. A modified feedforward hybrid active noise control system for vehicle[J]. Applied Acoustics, 2021, 175: 107816.

[29] LIU J, LIU S Y, LI M H. An error separation module with variable momentum algorithm for narrowband active noise control[J]. Applied Acoustics, 2025, 228: 110366.

[30] HUSH D, AHMED N, DAVID R, et al. An adaptive IIR structure for sinusoidal enhancement, frequency estimation, and detection[J]. IEEE Transactions on Acoustics, Speech, and Signal Processing, 1986, 34(6): 1380-1390.

[31] XIAO Y G. A new efficient narrowband active noise control system and its performance analysis[J]. IEEE Transactions on Audio, Speech, and Language Processing, 2011, 19(7): 1865-1874.

[32] NEHORAI A. A minimal parameter adaptive Notch filter with constrained poles and zeros[J]. IEEE Transactions on Acoustics, Speech, and Signal Processing, 1985, 33(4): 983-996.

[33] IRANPOUR M, LOGHMANI A, DANESH M. Active noise control for global broadband noise attenuation in a cylindrical cavity using modal FxLMS algorithm[J]. Journal of Vibration and Control, 2024, 30(1/2): 266-277.

Acknowledgement This work was supported in part by the Postgraduate Research & Practice Innovation Program of Nanjing University of Aeronautics and Astronautics (No.xcxjh20240326).

Authors

The first author Mr. **PANG Mingrui** is currently a candidate for a master of engineering degree at Nanjing University of Aeronautics and Astronautics. His research interests focus on the active noise control, adaptive signal processing.

The corresponding author Dr. **LIU Jian** received his B.S., M.S., and Ph.D. degrees in instrumentation science and technology from Harbin Institute of Technology, Harbin, China. He is now a lecturer of Nanjing University of Aeronautics and Astronautics, Nanjing, China. His main interests of research are in active noise control, adaptive signal processing, and array signal processing.

Author contributions Mr. **PANG Mingrui** designed the study, carried out the literature review, conducted the analysis, interpreted the results, drafted the initial manuscript and revised the manuscript. Ms. **LIU Yifei** conducted the experiments, collected and visualized data. Dr. **LIU Jian** contributed to the discussion and background of the study, supervised the project. All authors commented on the manuscript draft and approved the submission.

Competing interests The authors declare no competing interests.

(Production Editor: WANG Jie)

一种具有窄带频率自适应估计和误差分离的前馈混合有源噪声控制系统

庞明睿，刘亦菲，刘　剑

(南京航空航天大学自动化学院，南京 211106，中国)

摘要：传统的前馈混合主动噪声控制(Feedforward hybrid active noise control, FFHANC)系统结合了前馈窄带主动噪声控制(Feedforward narrowband active noise control, FFNANC)系统与前馈宽带主动噪声控制(Feedforward broadband active noise control, FFBANC)系统的优势。为提升其在频率失配(Frequency mismatch, FM)条件下的自适应调节能力，本文在传统FFHANC系统中引入了一种窄带频率自适应估计模块。该模块结合了自回归(Autoregressive, AR)模型与线性级联自适应陷波滤波器(Linear cascaded adaptive notch filter, LCANF)，能够在显著FM条件下实现精确的参考信号频率估计。此外，针对传统FFHANC系统中误差信号的窄带与宽带分量与其对应控制滤波器间相干性不足的问题，提出了一种基于自回归带通滤波器组(Autoregressive bandpass filter bank, AR-BPFB)的误差分离算法。仿真结果表明，所提出的FFHANC系统在高FM条件下仍能保持稳健性能，并有效抑制混合频带噪声；所提出的AR-BPFB算法显著提升了FFHANC系统的收敛速度。

关键词：主动噪声控制；前馈混合主动噪声控制系统；自回归模型；线性级联自适应陷波滤波器；带通滤波器组；误差分离